



## Open Archive Toulouse Archive Ouverte (OATAO)

OATAO is an open access repository that collects the work of Toulouse researchers and makes it freely available over the web where possible.

This is an author -deposited version published in: <http://oatao.univ-toulouse.fr/Eprints ID: 3455>

**To link to this article:** DOI:10.1016/S0022-1694(00)00391-7

**URL:** [http://dx.doi.org/10.1016/S0022-1694\(00\)00391-7](http://dx.doi.org/10.1016/S0022-1694(00)00391-7)

Ladouche, B. and Probst, Anne and Viville, D. and Idir, S. and Baqué, David and Loubet, M. and Probst, Jean-Luc and Bariac, T. ( 2001) *Hydrograph separation using isotopic, chemical and hydrological approaches (Strengbach catchment, France)*. Journal of Hydrology, vol. 242 (n° 3-4). pp. 255-274.

Any correspondence concerning this service should be sent to the repository administrator:  
[staff-oatao@inp-toulouse.fr](mailto:staff-oatao@inp-toulouse.fr)

# Hydrograph separation using isotopic, chemical and hydrological approaches (Strengbach catchment, France)

B. Ladouche<sup>a</sup>, A. Probst<sup>b,c</sup>, D. Viville<sup>d</sup>, S. Idir<sup>b</sup>, D. Baqué<sup>c</sup>, M. Loubet<sup>c</sup>, J.-L. Probst<sup>b,c</sup>,  
T. Bariac<sup>a,\*</sup>

<sup>a</sup>Laboratoire de Biogéochimie Isotopique, LBI/UPMC/CNRS/INRA, Case 120, 4 Place Jussieu, 75252 Paris, France

<sup>b</sup>Centre de Géochimie de la Surface, CGS/CNRS, 1, Rue Blessig, 67084 Strasbourg Cedex, France

<sup>c</sup>Laboratoire des Mécanismes de Transfert en Géologie, LMTG/UPS/CNRS, 38 rue des Trente-Six-Ponts, 31400 Toulouse, France

<sup>d</sup>Centre d'Etudes et de Recherches Eco-Géographiques, CEREG/ULP/CNRS, 3 rue de l'Argonne, 67083 Strasbourg Cedex; France

The streamflow components were determined in a small catchment located in Eastern France for a 40 mm rain event using isotopic and chemical tracing with particular focus on the spatial and temporal variations of catchment sources.

Precipitation, soil solution, springwater and streamwaters were sampled and analysed for stable water isotopes (<sup>18</sup>O and <sup>2</sup>H), major chemical parameters (SO<sub>4</sub><sup>2-</sup>, NO<sub>3</sub><sup>-</sup>, Cl<sup>-</sup>, Na<sup>+</sup>, K<sup>+</sup>, Ca<sup>2+</sup>, Mg<sup>2+</sup>, NH<sub>4</sub><sup>+</sup>, H<sup>+</sup>, H<sub>4</sub>SiO<sub>4</sub>, alkalinity and conductivity), dissolved organic carbon (DOC) and trace elements (Al, Rb, Sr, Ba, Pb and U). <sup>18</sup>O, Si, DOC, Ba and U were finally selected to assess the different contributing sources using mass balance equations and end-member mixing diagrams.

Isotopic hydrograph separation shows that the pre-event water only contributes to 2% at the beginning of the stormflow to 13% at the main peak flow. DOC associated to Si and U to Ba allow to identify the different contributing areas (upper layers of the saturated areas, deep layers of the hillslope and rainwater). The streamflow (70%) originates from the deep layers of the hillslope, the remaining being supplied by the small saturated areas.

The combination of chemical (both trace and major elements) and isotopic tracers allows to identify the origin of water pathways. During the first stage of the storm event, a significant part of the runoff (30–39%) comes from the small extended saturated areas located down part of the basin (overland runoff then groundwater ridging). During the second stage, the contribution of waters from the deep layers of the hillslope in the upper subcatchment becomes more significant. The final state is characterised by a balanced contribution between aquifers located in moraine and downslopes.

Indeed, this study demonstrates the interest of combining a variety of hydrometric data, geochemical and isotopic tracers to identify the components of the streamwater in such conditions. © 2001 Elsevier Science B.V. All rights reserved.

**Keywords:** Hydrograph separation; <sup>18</sup>O; Dissolved organic carbon; Si; U; Ba; Small catchment; Event water; Contributive areas

## 1. Introduction

In recent years, geochemical methods and environmental isotope techniques have been used increasingly to determine streamflow components in various catchments under different environmental conditions (for example, Pinder and Jones, 1969;

\* Corresponding author. Tel.: +33-1-4427-5998; fax: +33-1-4427-4164.

E-mail addresses: aprobst@cict.fr (A. Probst), viville@geographie.u-strasbg.fr (D. Viville), sidir@illite.u-strasbg.fr (S. Idir), loubet@lucid.ups-tlse.fr (M. Loubet), jlprobst@cict.fr (J.-L. Probst), bariac@ccr.jussieu.fr (T. Bariac).

Sklash and Farvolden, 1979; Hooper and Shoemaker, 1986; Maulé and Stein, 1990; McDonnell et al., 1990). So, there have been numerous studies on the mechanism of streamflow generation and hydrograph separation analysis. Generally, these studies used an approach based on a two or three-component mixing model representing conservation of mass describing the amount of water and isotope tracers from rainfall (event water) and pre-event water in the stream hydrograph of the event. This approach identifies the temporal origin of streamflow components but cannot be used to assess the spatial origin. Thus, the separation of contributions of water circulating in both the deep and superficial parts of a potential source with vertical chemical zonation can only be elucidated by chemical tracers, if the selected tracers behave conservatively. To obtain both temporal and spatial origins, some investigations using stable isotopes associated with chemical tracers, have been undertaken in several different basins (for example, Hooper and Shoemaker, 1986; Kennedy et al., 1986; Wels et al., 1991; Durand et al., 1993; Laudon and Slaymaker, 1997).

However, several conditions have to be fulfilled as defined by Sklash and Farvolden (1979) as debated, for instance, in Kennedy et al. (1986), Rodhe (1987), McDonnell et al. (1990), Kendall and McDonnell (1993) and Buttle (1994). Briefly, in order to perform the hydrograph separation, the following major assumptions are generally made: (1) the main components of streamflow are isotopically and geochemically distinguishable; (2) the geochemical composition of streamflow components remains constant with time; and (3) groundwater and soil water (pre-event water) are geochemically equivalent. However, these assumptions are rarely tested since the spatial and temporal sampling of water from different components is difficult.

In the present study, we examined the spatial and temporal variations of catchment source waters using a variety of isotopic and geochemical tracers and also hydrological measurements in order to identify and characterise stormflow components and their respective contribution to the streamflow outlet.

## 2. Study area

The Strengbach, a second-order stream with a

catchment area of  $0.8 \text{ km}^2$ , is located in the Vosges Mountains (Eastern France, Fig. 1), ranges from 883 to 1146 m above sea level, with highly incised side slopes (mean  $15^\circ$ ). Viville et al. (1988) and Probst et al. (1990) provided a detailed site description of this catchment. Relevant aspects are summarised below. The substratum is mainly composed of a base-poor leucogranite. At the northern top edge, the granite is in contact with a banded gneiss. Podzolic and brown acidic soils are generally less than 1 m thick, and overlie coarse-textured tills developed to a thickness ranging from 1 to 9 m. The catchment, with the exception of the valley bottom, is completely forested. About seventy percent of the cover is Norway spruce (*Picea abies* L.): the remainder consists of mixed white fir (*Abies alba* Mill.) and beech (*Fagus sylvatica* L.). Spruce stands are affected by crown-thinning and yellowing attributed to Mg deficiencies and partially to water stress periods during the 1970–1990 period (Landmann and Bonneau, 1995).

The climate is temperate oceanic mountainous. The mean annual temperature is  $6^\circ\text{C}$ . Mean annual rainfall is of 1400 mm evenly well distributed through the year and ranges between 1100 and 1600 mm over the period 1986–1995 (Probst and Viville, 1997). The mean annual runoff for the corresponding period on the Strengbach is of 850 mm ( $26.9 \text{ l s}^{-1} \text{ km}^{-2}$ ). A second-order hyperbolic function fits the recession curve. The storage capacity of the well-drained shallow aquifer is estimated to 100 mm for a specific discharge of  $114 \text{ l s}^{-1} \text{ km}^{-2}$  (Latron, 1990). In the valley bottom, a surface saturated area is connected to the drainage pattern. Its extent ( $S$ , ha) — mapped for different hydrologic status — is well related to the stream baseflow ( $Q$ ,  $\text{l s}^{-1}$ ):

$$S = 1.15 \log Q - 0.13 \quad (1)$$

with  $n = 14$  and  $r^2 = 0.944$ .

The maximum extent of the surface saturated area represents only 3% of the total catchment area for a stream baseflow of  $114 \text{ l s}^{-1} \text{ km}^{-2}$  (Latron, 1990).

## 3. Materials and methods

### 3.1. Instrumentation

The catchment has been instrumented since 1986

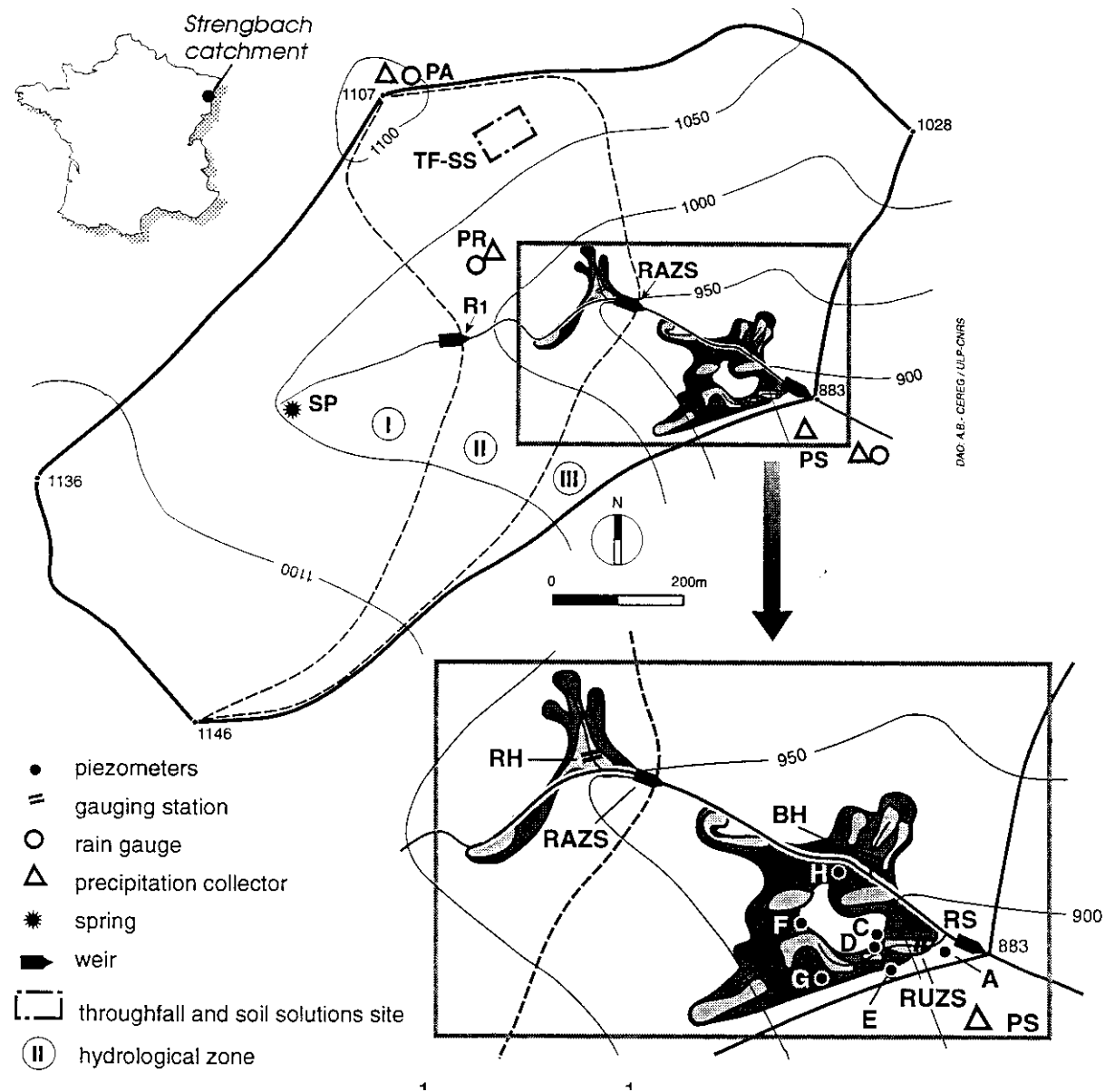


Fig. 1. Location map of the study area and of sampling sites.

with an extensive array of hydrologic equipment (Viville et al., 1988; Probst et al., 1990, Fig. 1). A H-flume type continuously gauges the stream discharge at the outlet (site RS). Water levels are measured to  $\pm 1$  mm with an ultrasonic type transducer and recorded by a CR2M system (CR2M company, France). For the present study, the Strengbach main brook is also gauged — from upstream to downstream — by two other flumes (named R1, RAZS), which define, respectively, two subcatchments (called I and II), of 0.291 and 0.546 km<sup>2</sup>, respectively. Hydrological zones included between gauging stations are called, respectively, from up stream to down stream, Zone I, Zone II and Zone III (Fig. 1). They are defined as follows:

- Zone I = Subcatchment I = 0.291 km<sup>2</sup>
- Zone II = Subcatchment II – Subcatchment I = 0.255 km<sup>2</sup>
- Zone III = Whole catchment – Subcatchment II = 0.254 km<sup>2</sup>.

In hydrological zones II and III, sites BH and RH are gauging stations on first-order rills which drain a part of the south-facing hillslope. In zone III, site RUZS drains a part of the upper layers of the saturated area. Differential gauging measurements between sites RAZS and R1 and between the outlet (RS) and site RAZS allow to quantify both contributions of zones II and III and also ungauged flow (non-point flow:  $Q_X$ ) from these zones:

$$Q_{XII} = Q_{RAZS} - (Q_{R1} + Q_{RH}) \quad (2)$$

$$Q_{XIII} = Q_{RS} - (Q_{RAZS} + Q_{BH} + Q_{RUZS}) \quad (3)$$

During the stormflow period 18–20 May 1994, surface waters from the main stream (sites RS, RAZS and R1) and tributaries (sites RH, BH and RUZS) have been gauged and sampled simultaneously. Samples were collected by hand. At the outlet (RS), the water sampling frequency has been suited to the discharge temporal evolution (from 4 to 30 min). Manual gauging and water sampling of others sites (RAZS, R1, RUZS, BH and RH) were adapted to the outlet one.

The sampling network includes three rainfall gauges (type SPIEA 400 cm<sup>2</sup>) installed along an altitudinal transect (sites PS: 880 m, PR: 1010 m and PA:

1100 m, Fig. 1) to determine the variations in geochemical and isotopic compositions, and rainfall amount of open field precipitation at the catchment scale. Rainfall samples were intensively collected by hand with various time intervals (4, 8, 20 or 30 min). Throughfall (TF) under a mature spruce stand (which is the dominant vegetation cover) was collected using two 2 m long gutter collectors located below the spruce canopy. TF sampling was performed at 10 min intervals during rainfall event.

In subcatchment I, springwater has been collected at site SP at various times during the study together with discharge. In subcatchment III, the isotopic and chemical characteristics of pre-event water (before stormflow) have been determined using seven shallows piezometers and two pits located in the upper part of the saturated area (Fig. 1). Water table levels in piezometer network have been measured prior and during stormflow period by portable well reading accurate to 1 cm. Prior the streamflow, soil sample cores have been collected in the vicinity of the shallow piezometer network in the subcatchment III.

Soil samples were collected at 0.05 m intervals to a depth of 0.2 m and then with 0.1 m intervals to a depth of 1 m. Water extracted from soil sample cored was performed by the vacuum distillation method. During the storm event, soil solutions (SS) were collected at various depths (–0.5, –0.10, –0.30 and –0.60 m) using zero-tension lysimeters located in the upper part of the south-facing slope hillslope (site SS, Fig. 1).

### 3.2. Sample collection and chemical analysis

Major chemical parameters pH, electrical conductivity, alkalinity, silica, SO<sub>4</sub><sup>2–</sup>, NO<sub>3</sub><sup>–</sup>, Cl<sup>–</sup>, Na<sup>+</sup>, K<sup>+</sup>, Ca<sup>2+</sup>, Mg<sup>2+</sup>, NH<sub>4</sub><sup>+</sup>, dissolved organic carbon (DOC), as well as trace elements (Al, Rb, Sr, Ba, Pb and U) and stable water isotopes (<sup>18</sup>O and <sup>2</sup>H) were analysed. Samples were collected in polyethylene bottles and filtered through 0.45 µm Millipore membrane for major element analyses. For trace elements, samples were collected in polypropylene bottles, filtered through 0.2 µm Millipore membranes and acidified using a 2% weight HNO<sub>3</sub> solution. Analyses were performed within a few days after sampling. Base cations (Na<sup>+</sup>, K<sup>+</sup>, Ca<sup>2+</sup>, Mg<sup>2+</sup>) were analysed by atomic absorption spectrophotometry, strong acid

anions ( $\text{SO}_4^{2-}$ ,  $\text{NO}_3^-$ ,  $\text{Cl}^-$ ), by ion chromatography (Dionex apparatus), dissolved silica ( $\text{H}_4\text{SiO}_4$ ) and ammonium ( $\text{NH}_4^+$ ) by automatic colorimetry (Technicon II apparatus). Alkalinity was measured by Gran's titration (pH range 3.0–4.04 single step procedure). DOC analysis was performed with a Shimadzu TOC 5000-analyser.

Trace elements were analysed using an ICP-AES and ICP-MS techniques. Analytical precision varies as a function of the absolute element content. It was estimated to vary from  $\pm 5\%$  for elements with concentrations higher than 2 ppb to  $\pm 20\%$  for element contents lower than 0.2 ppb.

Measurements of oxygen isotopic composition of the water samples were carried out using the standard  $\text{CO}_2$  equilibration method (Epstein and Mayeda, 1953). Water samples were prepared for measurements of deuterium by reduction of water to hydrogen over zinc at  $540^\circ\text{C}$  following the standard method (Coleman et al. 1982). Stable isotope ratios were determined using a VG Optima mass spectrometer. Isotopic ratios are reported in the  $\delta$  notation (as ‰) relative to the Vienna-Standard Mean Ocean Water (V-SMOW, Gonfiantini, 1978):

$$\delta = \left( \frac{R_{\text{sample}}}{R_{\text{SMOW}}} - 1 \right) 10^3 \quad (4)$$

where  $R$  is the ratio  $^{18}\text{O}/^{16}\text{O}$  or  $^2\text{H}/^1\text{H}$ . Standard deviations are 0.05 and 1‰, respectively.

### 3.3. Hydrograph separation

The well-established two to  $n$ -component mixing model (Pinder and Jones, 1969) is used to separate the streamflow components. This approach based on two mass conservations — one for water and one for the geochemical tracer — allows to separate the relative contribution of the different components which correspond to different reservoirs or to different contributive areas. The use of isotopic tracers allows to separate the runoff hydrograph into pre-event water (stored in the catchment prior the storm event: soil water, groundwater) and event water (brought by the rainfall event) while the use of geochemical tracers allows to identify the three-dimensional origins of the stormflow components. The respective contributions of  $Q_1$  and  $Q_2$  components to streamflow  $Q_s$  can be calculated by using the two following mass balance

equations:

$$Q_s = Q_1 + Q_2 \quad (5)$$

$$Q_s C_s = Q_1 C_1 + Q_2 C_2 \quad (6)$$

Where  $Q$  is the discharge and  $C$  the concentration. Subscripts  $s$ , 1 and 2 refer to streamflow, components 1 and 2, respectively.

The relative contribution of components 1 and 2 can be calculated, at any given time from Eqs. (5) and (6), if the total discharge  $Q_s$  and concentrations  $C_s$ ,  $C_1$  and  $C_2$  are known:

$$Q_2 = \frac{C_s - C_1}{C_2 - C_1} Q_s \quad (7)$$

$$Q_1 = Q_s - Q_2 \quad (8)$$

## 4. Results

### 4.1. Hydrology, isotopic and chemical characteristics

#### 4.1.1. Hydrological response to storm

The main hydrological characteristics of the event of 18–20 May 1994, are summarised in Table 1. The two successive rainfall events (27 and 14 mm) are characterised by low rainfall rate (average intensity  $< 3 \text{ mm h}^{-1}$ ). This type of rainfall event is of a relatively common occurrence in the north-eastern France during springtime (approximately 1 year return period). For the whole catchment, the total rainfall ranges from 40 to 43 mm depending on sites. Average rainfall amount is estimated about 40.6 mm (i.e. volume of precipitation,  $V_p = 32\,540 \text{ m}^3$ ).

The storm of 18–19 May 1994, follows a relatively dry period; discharge at the outlet is low ( $7.21 \text{ s}^{-1}$ , Table 1) and flow at site R1 had ceased. The main feature of hydrographs is the close coincidence of discharge peaks between the different sites (Fig. 2), and also the relationship between peaks of discharge with increasing rainfall intensity. Stream discharge at the outlet (RS) increases regularly up to  $28 \text{ l s}^{-1}$ ; after the first peak reached at 21:00 hours discharge follows rainfall intensity variations and the maximum measured peakflow is of  $34.71 \text{ l s}^{-1}$  at 0:22 hours (19th May). During the second storm, two other main peaks of  $28 \text{ l s}^{-1}$  are monitored at 05:30 hours and 09:00 hours, respectively. Later, the rain intensity

Table 1

Main hydrological characteristics of the 18–20th May storm event (initial extent of saturated area:  $S = 1.1\%$  of the catchment area (i.e. 8800 m<sup>2</sup>), value calculated by Eq. (1) with  $Q = 7.2 \text{ l s}^{-1}$ ; final extent of saturated area:  $S = 1.5\%$  of the catchment area (i.e. 12 000 m<sup>2</sup>), value calculated by Eq. (1) with  $Q = 13.6 \text{ l s}^{-1}$

	Outlet RS ( $A = 0.8 \text{ km}^2$ )	Site RUZS	Site BH	Site RAZS ( $A = 0.546 \text{ km}^2$ )	Site RH	Site R1 ( $A = 0.291 \text{ km}^2$ )
Base flow ( $\text{l s}^{-1}$ )	7.2	0.3	0.6	4.5	0.7	0
Main peak flow ( $\text{l s}^{-1}$ ) — event no. 1	34.7	7.8	2.6	9.3	1.4	1.31
Main peak flow ( $\text{l s}^{-1}$ ) — event no. 2	28.0	5.3	1.9	11.0	1.32	2.46
Final discharge	13.6	0.6	0.7	6.9	0.7	0.3
Total stormflow (m <sup>3</sup> )	2483	375	189	1026	144	136
Quickflow: QF (m <sup>3</sup> )	1127	317	87	307	36	114
QF/P (%)	3.46	1	0.3	1.0	0.1	0.3

becomes lower than  $1 \text{ mm h}^{-1}$  and the stream discharge decreases regularly down to  $13.6 \text{ l s}^{-1}$  on 20th May.

Water table readings indicate a general water level raising between 18 and 19th May, with a 0.4 m value in the saturated zone (D) (Fig. 3). The piezometers located in the upper slope of this area (F and G) indicate a maximum water level early in the morning of 19th May. Then, a decrease is observed whereas the water level of the down slope piezometer (A) continues to raise and reaches a maximum at 16:00 hours, which indicates downwards wave propagation on this slope (Fig. 3).

#### 4.1.2. Isotopic compositions of waters

##### (a) Isotopic signature of pre-event water

Deep and shallow groundwater, soil water, TF and

streamwater samples are distributed along the local meteoric water line in a  $\delta^2\text{H}$ – $\delta^{18}\text{O}$  diagram:

$$\delta^2\text{H} = 8.3(\pm 0.2) \delta^{18}\text{O} + 11.3(\pm 1.8) \quad (9)$$

with  $n = 53$ ,  $r = 0.96$ .

This suggests that soil water and groundwater are not affected by evaporation processes during infiltration owing to the presence of an important vegetation cover (Millet et al., 1998): the leaf area index for a stand composed of 30-year-old Norway spruce is of  $6.6 \pm 0.4$  (Biron, personal communication). So, streamflow components (soil water and groundwater) have a signal that results from a mixture of new rainwater and old rainwater, stored in the catchment prior the stormflow event: the rain seeps through the soil and

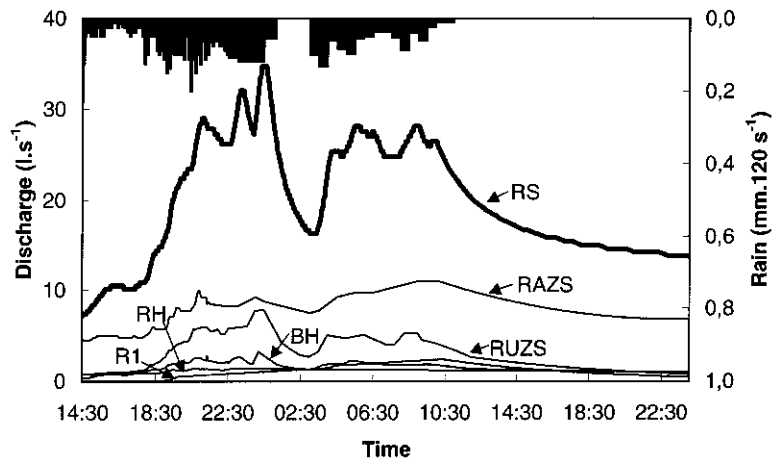


Fig. 2. Hyetogram and hydrographs of the Strengbach and its tributaries during the 18–20th May storm event.

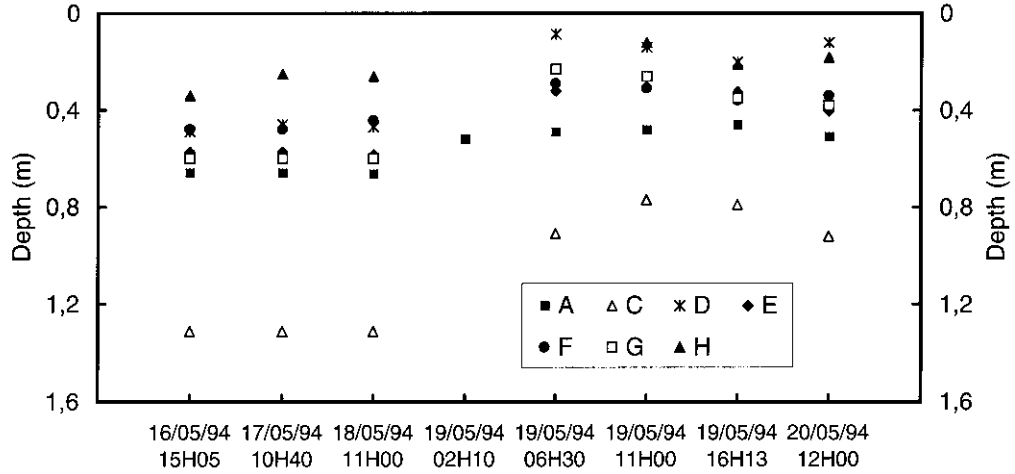


Fig. 3. Variations of water depths in the different piezometers of the saturated area during the 18–20th May storm event.

the unsaturated zone, and mixed up with non-evaporated water from older rains.

The isotopic compositions ( $\delta^{18}\text{O} = -9.5\text{‰}$ ,  $\sigma = 0.3\text{‰}$ ,  $n = 6$ ) of the unsaturated soil water collected in the vicinity of the piezometer 'A' (Fig. 1) is very close to the one ( $\delta^{18}\text{O} = -9.4\text{‰}$ ) measured in the shallow piezometer 'A' before the stormflow event: there is no evaporation in the soil water, and root absorption and capillary rise do not lead to isotope fractionation (Zimmerman et al., 1967).

The groundwater samples collected from the piezometer network at various depths (0.5–1.3 m range) indicate that the shallow groundwater system localised in the lower part of zone III has an homogeneous isotopic concentration (mean  $\delta^{18}\text{O}$  value =  $-9.50\text{‰}$ ,  $\sigma = 0.10\text{‰}$ ,  $n = 7$ ). The deep groundwater system, characterised by spring water (zone I) has also a uniform isotopic composition with a mean value of  $-9.7 \pm 0.2\text{‰}$  ( $n = 4$ ). Differences between the mean  $\delta^{18}\text{O}$  values of shallow and deep groundwater system are not statistically significant. At the catchment scale, the isotopic variability of groundwater prior to the stormflow period is negligible.

The oxygen-18 content of streamwater during baseflow condition ( $-9.45\text{‰}$ ) is similar to the mean isotopic composition of groundwater ( $-9.5\text{‰}$ ), suggesting that stream baseflow is composed exclusively of groundwater. Consequently, groundwater flow controls baseflow and the isotopic composition of

the stream baseflow can be used to characterise the pre-event component.

#### (b) Isotopic signature of rain water

The storm event was sampled intensively. The main feature is the large temporal evolution of the  $\delta^{18}\text{O}$  values in the rainfall (Fig. 4). The  $\delta^{18}\text{O}$  values of the first rainfall event ranges more than  $9\text{‰}$  ( $-3.8$  to  $13\text{‰}$ , Table 2) whereas the second rainfall ranges from  $-9.7$  to  $-6.6\text{‰}$ . The bulk  $\delta^{18}\text{O}$  values for the first and the second rainfall events are  $-10.9$  and  $-8.2\text{‰}$ , respectively. For the whole rainfall event (first + second storm event), the bulk rainfall  $\delta^{18}\text{O}$  value is  $-10.1\text{‰}$ .

Owing to the wide temporal variation of isotopic contents, the selection of appropriate isotopic composition of event water for isotopic hydrograph separation has been performed using the cumulative incremental weighting approach based on rainfall amount as recommended by McDonnell et al. (1990).

$$\delta^{18}\text{O}_{\text{event water}(i)} = \frac{\sum_{i=1}^n \delta^{18}\text{O}_i}{\sum_{i=1}^n P_i} \quad (10)$$

where  $P_i$  and  $\delta^{18}\text{O}_i$  are the precipitation amount collected fractionally, and its oxygen isotope concentration, respectively.

However, this method only considers the  $\delta^{18}\text{O}$



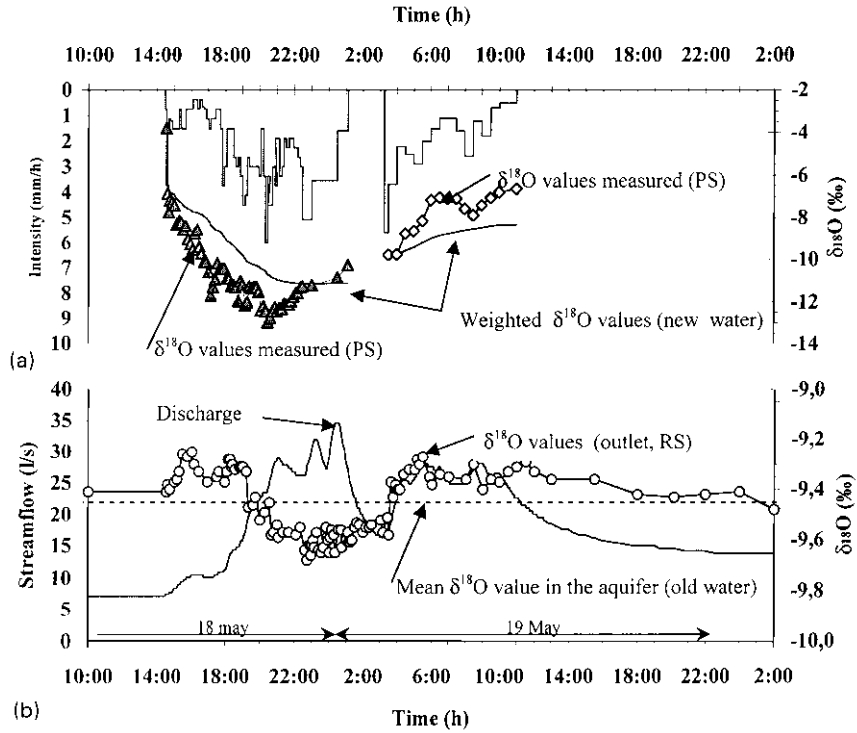


Fig. 4. Variations of  $\delta^{18}\text{O}$  in rainfall (a) and in the stream at the outlet (b) compared with rain (a) and discharge variations (b) during the 18–20th May storm event.

value of the rain, which had occurred before the time of stream sampling and gives greater weighting to episodes of higher intensity rain within storms which may produce a large rapid runoff response.

For the first rainfall event, the  $\delta^{18}\text{O}$  values of new water calculated using Eq. (10) show considerable variation (more than 7‰) between the beginning and the end of the storm (Fig. 4). The values of event water fluctuate from  $-3.8$  to  $-10.9$ ‰ and from  $-9.7$  to  $-8.2$ ‰ for the first and the second rainfall events, respectively.

The event water isotopic composition calculated for each rainfall gauge (sites PS, PR and PA) is very similar. The gradients of the altitude effect are of 0.13 and 0.17‰ per 100 m elevation increase for the two rainfall events, respectively. Therefore, the spatial variation of  $\delta^{18}\text{O}$  in open field precipitation can be ignored because its range is negligible compared to those of the temporal variation (7 and 1.5‰ for the first and the second rainfall event, respectively).

(c) Isotopic signature of the surface waters during the event

During the stormflow period, sampling of the groundwater indicates a constant isotopic signature. The isotopic content of the streamflow (RS) oscillates around the  $\delta^{18}\text{O}$  value of groundwater and returns to the initial value during the recession stage (Fig. 4). The  $\delta^{18}\text{O}$  value of the two other stream gauging stations (RAZS, R1) and tributary rills (sites RUZS, BH and RH) shows a similar temporal evolution to that measured at the outlet. So, spatial variability of the isotopic composition of streamwater is fairly small at the catchment scale, considering the uncertainty. In addition, the  $\delta^{18}\text{O}$  values of streamwater show a low variation (0.5‰) compared to those observed in the open field precipitation (Fig. 4). This indicates that the event water contribution to the runoff is not important.

#### 4.1.3. Geochemical composition of the waters

During the storm event, open field precipitation is slightly acidic (mean pH of 5.1), and very low

Table 2

Mean, standard deviation, maximum, minimum values for the main chemical parameters in rainwater (PS), Stream water (RS, RAZS), Springwater (SP) and different tributaries (RH, BH, RUZS) during the storm event. All data are expressed in  $\mu\text{mol l}^{-1}$ , except DOC in  $\text{mg l}^{-1}$ , Al, Ba, Rb, Sr, Pb in  $\mu\text{g l}^{-1}$ , U in  $\text{ng l}^{-1}$  and conductivity (Cond.) in  $\mu\text{S cm}^{-1}$ ,  $^{18}\text{O}$  in ‰; <: below detection limit

	PS <sup>a</sup>				TF <sup>b</sup>				RUZS <sup>c</sup>				RH <sup>d</sup>				BH <sup>e</sup>				RS <sup>f</sup>				RAZS <sup>g</sup>				SP <sup>h</sup>					
	Mean	SD	Min	Max	Mean	SD	Mini	Max	Mean	SD	Mini	Max	Mean	SD	Mini	Max	Mean	SD	Mini	Max	Mean	SD	Mini	Max	Mean	SD	Mini	Max	Mean	SD	Mini	Max		
δ <sup>18</sup> O	-10.1	1.9	-13	-3.8					-9.4	0.2			-9.7	-9.1	-9.4	0.1	-9.5	-9.3	-9.4	0.1	-9.7	-9.3	-9.5	0.1	-9.5	-9.3	-9.5	0.1	-9.6	-9.5				
Cond.	7.8	6.4	3	33	41.1	20.9	4.9	84.4	13.7	0.7			12.3	15	37.7	5.1	21.5	43	37.0	0.9	34.7	39.1	28.3	2.6	24	33	33.7	2.1	30.4	36.5	36.2	0.0	36.2	36.2
H <sup>+</sup>	7	9.8	1	39	25	23.7	0.1	93.3	1.1	0.2			0.7	1.6	0.45	0.1	0.3	0.5	0.2	0.02	0.2	0.3	0.6	0.07	0.4	0.7	0.7	0.07	0.6	0.9	0.6	0.06	0.6	0.7
NH <sub>4</sub> <sup>+</sup>	21	22.7	5	112	93	107	8	518	<	-			<	<	<	-	<	<	<	-	<	<	<	<	-	<	<	<	-	<	<	<	<	
Na <sup>+</sup>	3	2	1	7	20	16.9	1	87	27	3.5			22	34	78	4.8	72	87	81	3.9	73	87	62	7.4	51	78	76	3.2	70	82	82	0.8	81	83
K <sup>+</sup>	2	1.5	1	6	57	44.4	1	230	2	1.1			1	4	22	1	20	23	18	1.4	15	20	12	0.8	11	14	17	0.4	17	18	19	0	19	19
Mg <sup>2+</sup>	2	0.9	1	4	9	4.7	1	17	10	0.5			9	10	31	2	28	34	39	0.8	37	40	21	2.0	18	24	24	1.1	23	26	20	0	20	20
Ca <sup>2+</sup>	5	4.4	1	20	38	22.5	1	76	40	1.4			37	42	90	5.2	83	99	86	1.6	83	88	64	4.6	55	73	76	3.2	70	80	76	0	76	76
Al	4	2	2	7	39	23	12	76	159	9			148	173	40	8	31	57	46	14	28	66	61	25	31	103	42	12	31	61	16	2.6	14	18
Ba	2.2	1.2	0.7	3.3	5.1	2.6	1.3	8.3	23.4	1.2			21.4	25.5	122.1	2.0	119.0	124.3	69.2	1.9	66.7	72.3	62.1	8.2	50.2	82.1	92.0	12.2	80.5	105.7	69.1	0.03	69.1	69.2
Rb	0.5	0.4	0.08	1.1	13.7	11.9	3.2	35.8	0.5	0.1			0.3	0.7	2.7	0.1	2.7	2.9	2.2	0.3	1.8	2.7	1.7	0.2	1.5	2.2	2.6	0.3	2.3	2.9	2.7	0.03	2.7	2.8
Sr	1.8	1.2	0.4	3.3	4.6	2.6	0.8	7.4	6.5	0.3			6.1	6.8	14.1	0.2	13.8	14.5	10.6	0.2	10.3	11.0	10.4	1.2	8.6	13.3	13.6	1.9	12.0	15.9	11.2	0.04	11.1	11.2
Pb	0.11	0.06	0.06	0.20	1.76	0.82	0.56	3.11	0.64	0.11			0.47	0.78	0.07	0.09	0.03	0.27	0.11	0.05	0.04	0.20	0.18	0.08	0.06	0.30	0.08	0.02	0.04	0.09	0.02	0.01	0.01	0.02
U	7	1	6	7	12	8	5	28	41	3			36	44	130	8	120	140	100	20	80	130	210	60	140	320	160	40	130	240	157	30	136	178
Alk. + H <sup>+</sup>	5	8.2	0	32	4	14.1	0	61	32	4.7			26	42	44	4.6	35	49	95	4.3	86	102	38	2.0	34	43	28	3.4	23	34	36	3.7	33	42
Cl <sup>-</sup>	3	2.2	1	9	32	23.5	1	111	2	1.1			1	4	43	5.1	37	52	39	2.7	34	43	29	4.7	22	40	41	2.9	36	46	43	0	43	43
NO <sub>3</sub> <sup>-</sup>	15	14.5	5	70	97	59.2	8	214	1	1			1	1	32	6.7	25	43	19	2.7	16	25	19	2.2	16	23	-34	0.9	32	35	34	0	34	34
SO <sub>4</sub> <sup>-</sup>	10	8.5	3	43	68	41.6	5	214	28	4.8			22	36	110	7.8	98	122	89	6.1	78	100	72	9.7	55	90	91	5.2	82	101	89	1	88	90
H <sub>4</sub> SiO <sub>4</sub>	1	1	1	1	3	3.2	1	17	35	5.3			27	43	110	9.6	98	126	122	10	103	138	96	13.9	74	124	118	6.6	10.6	130	136	1.9	133	137
DOC	0.5	0.2	0.03	1.0	7.0	4.3	0.27	21.9	8.3	0.7			7.3	9.7	2.0	0.6	1.0	2.9	3.2	0.9	1.7	4.6	3.4	1.0	1.5	4.8	1.9	0.6	0.8	3	0.7	0.1	0.6	0.8

<sup>a</sup>  $n = 31$  except for  $^{18}\text{O}$  ( $n = 70$ ) and for trace elements ( $n = 4$ ).

<sup>b</sup>  $n = 84$  except for trace elements ( $n = 10$ ).

<sup>c</sup>  $n = 22$  except for  $^{18}\text{O}$  ( $n = 50$ ) and for trace elements ( $n = 8$ ).

<sup>d</sup>  $n = 14$  except for  $^{18}\text{O}$  ( $n = 17$ ) and for trace elements ( $n = 7$ ).

<sup>e</sup>  $n = 27$  except for trace elements ( $n = 13$ ).

<sup>f</sup>  $n = 43$  except for  $^{18}\text{O}$  ( $n = 103$ ) and for trace elements ( $n = 19$ ).

<sup>g</sup>  $n = 12$  except for  $^{18}\text{O}$  ( $n = 35$ ) and for trace elements ( $n = 5$ ).

<sup>h</sup>  $n = 4$  except for trace elements ( $n = 2$ ).

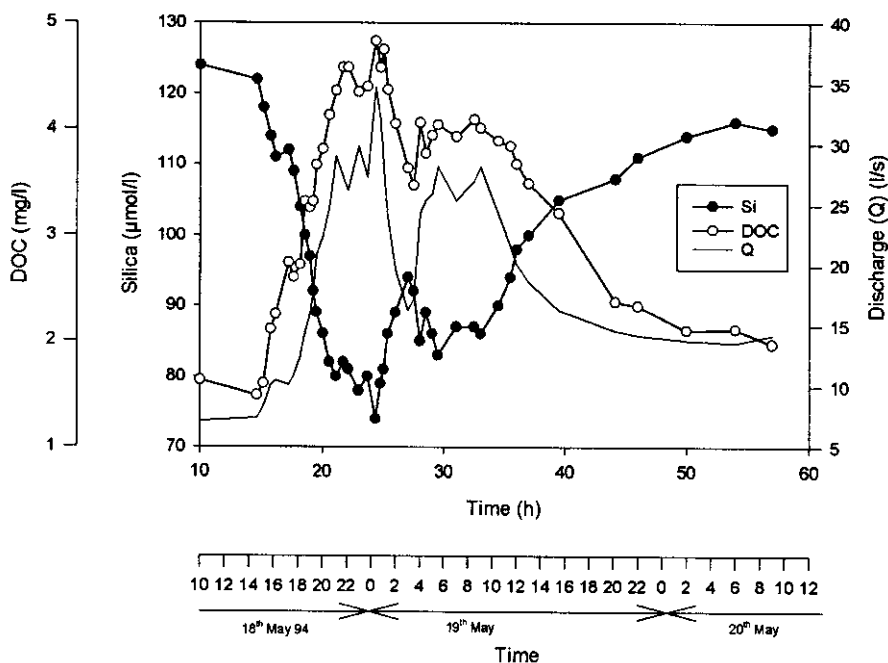


Fig. 5. Compared variations of DOC, silica and discharge in the Strengbach at the outlet during the 18–20th May storm event.

concentrated for major elements (less than  $10 \mu\text{mol l}^{-1}$ ) (Table 2). No significant difference of concentrations is observed between the different rain gauges. Ammonium, protons, sulphate and nitrate are dominant whereas dissolved silica and DOC are negligible as already observed in this catchment (Probst et al., 1990). Compared to surface waters, concentrations of trace elements are also very low, extending from some  $\mu\text{g l}^{-1}$  (Sr, Ba) to tens of  $\text{ng l}^{-1}$  (Pb) and to  $1 \text{ ng l}^{-1}$  (U). TF is more acidic than open field precipitation (mean pH of 4.6) and also more enriched in major elements than open field precipitation (ten to twenty-fold higher) as classically observed under spruce (Matzner, 1986; Probst et al., 1990, 1992) (Table 2). During the early part of the storm event, both open field precipitation and TF are strongly diluted; subsequently, rainfall is more acidic (mean pH of 4.4) and it is characterised by a significant increase of  $\text{SO}_4^{2-}$ ,  $\text{NO}_3^-$ ,  $\text{Cl}^-$  and  $\text{NH}_4^+$  concentrations: other elements remain negligible (Idir, 1998). Soil solutions are highly acidic and more acidic in surface horizons (0–10 cm; pH 3.6) than in the deep soil layers (30–60 cm; pH 4.3) (Dambrine et al., 1995). Moreover, dissolved silica,  $\text{Cl}^-$ ,  $\text{Ca}^{2+}$ ,  $\text{Mg}^{2+}$ , Sr and Ba concentrations increase with depth, whereas DOC, Rb,

Pb and U are more concentrated in surface horizons (0–10 cm depth).

Despite a significant input of acid precipitation, streamwater pH remains circumneutral (pH 6.0–6.7, Table 2), and decreases only weakly during the event, strengthening the important buffering capacity of the soil/saprolite compartment (cf. Probst et al., 1992; El Gh'Mari, 1995). This also indicates that the contribution of direct rainfall to streamflow is weak. As usual, calcium and sulphate are the dominant ions (cf. Probst et al., 1990). Four groups of chemical parameters can be identified depending on their chemical behaviour with respect to stream discharge at the outlet (RS) and at the upper subcatchment II (RAZS):

- Group I.  $\text{Na}^+$ ,  $\text{Ca}^{2+}$ ,  $\text{Mg}^{2+}$ , Ba, Sr (alkali-earth and alkali elements),  $\text{SO}_4^{2-}$ ,  $\text{Cl}^-$ ,  $\text{H}_4\text{SiO}_4$  (Fig. 5) and conductivity, which are strongly diluted with increasing discharge.
- Group II. K, Rb, pH and alkalinity for which concentrations are weakly diluted with rising discharge.
- Group III. DOC (Fig. 5), U and Pb of which contents increase with increasing discharge.

- Group IV.  $\text{NO}_3^-$  which is diluted during the first part of the flow event and concentrated in the second one.

At RAZS sampling site (upper subcatchment II), the variation range of concentrations is lower than at the stream outlet (RS, whole catchment) (Table 2).

Spring waters are also circumneutral and present similar chemical characteristics as streamwaters, however, they display a very low variation range of concentrations during the event (Table 2).

The patterns of concentrations in stream waters reflect the variable contributions of flow components to the stream during the event, according to the main origin of the chemical element.  $\text{Na}^+$ , Ba, Rb and silica are particularly enriched in waters draining deep horizons of the saprolite (spring water pattern) as a result of water–rock interaction and particularly of weathering of plagioclases and micas;  $\text{Ca}^{2+}$ ,  $\text{Mg}^{2+}$  and Sr originate both from atmospheric sources and mineral weathering within the soil and saprolite (Probst et al., 1992, 2000; El Gh'Mari, 1995).  $\text{Cl}^-$  and  $\text{SO}_4^{2-}$  originate essentially from the atmosphere but are concentrated within the catchment by evaporation processes and/or storage since no significant source of sulphide or chloride in bedrock was detected (Probst et al., 1992; 1995; El Gh'Mari, 1995). Other parameters like  $\text{K}^+$  and  $\text{NO}_3^-$  are strongly influenced by biological activity.

The saturated area drainage (RUZS) (Fig. 1) distinguishes clearly from the other sampling sites by different element concentration patterns. pH ranges between 6.1 and 5.8 and decreases weakly but regularly during the event, independently from discharge variations. RUZS is characterised by high DOC, U and Pb contents, low silica concentrations when compared to other sites, and it contains no nitrate (Table 2). DOC, U and Pb (which are strongly linked to organic matter compounds) increase significantly at the beginning of the storm event. Particularly, the DOC behaviour reflects the leaching of soil upper layers enriched in organic matter (Soulsby, 1992, 1995). Unlike the main stream and the other tributaries, RUZS concentration peaks of DOC,  $\text{Cl}^-$ ,  $\text{K}^+$ , Rb, U and Pb, as well as the maximum dilution of all the other major elements occur before the first peak of discharge.

The tributary BH (Fig. 1) presents intermediate concentration patterns between RS and RUZS.

## 4.2. Water contributions to streamflow

### 4.2.1. Hydrological zone contributions

This event is not very responsive: the total storm-flow ( $V_t$ ) is estimated to be  $2483 \text{ m}^3$  and a graphic hydrograph separation determines a direct runoff ( $V_c$ : 'quick flow' as defined by Hewlett and Hibbert, 1967) volume of  $1127 \text{ m}^3$  (i.e. 1.4 mm) whereas the remaining  $1357 \text{ m}^3$  is attributed to 'delayed flow'; quickflow then represents only 3.5% of the 40.6 mm rainfall. This result suggests that most of the rainfall is stored in the soils as indicated by measurements performed in the zero-tension lysimeters located in the upper hillslopes (site SS, Fig. 1). Indeed, the total soil water amount collected in the deeper lysimeter plates ( $-0.60 \text{ m}$ ) represents only 1 mm of the infiltrated rainfall. So, most of the infiltrated rainfall contributes to recharge the soil reservoir of the upper hillslopes.

Elsewhere, the measurements of drain and subcatchment discharges allow to quantify their respective contributions as well as relative contributions of hydrological zones to stream flow at the outlet. The trends in relative contributions can then be followed during the hydrological event. The respective contributions of the hydrological zones, as defined in Section 3.1, are evaluated according to four characteristic periods (pre-event state, first flood, second flood, and final state, Fig. 6).

At pre-event state, Zone II contribution represents 64% of the discharge at the outlet and there is no runoff in Zone I (Fig. 6). In Zones II and III (Fig. 1), ungauged flows ( $Q_{X_{II}}$  and  $Q_{X_{III}}$ , respectively) produce most of the runoff (as illustrated for Zone III in Fig. 7). During the first flood, the contribution of the down part of the catchment (Zone III) becomes essential and represents 65% of the flood at the outlet while the proportion of Zone II contribution decreases significantly (Fig. 6). In Zone I, at R1 site, stream begins to flow at 19:00 hours (i.e. 5:30 hours after the beginning of the rainfall event). During the second flood, the contributions of Zones III, II and I represent 57, 35 and 8% of the stream outlet flood, respectively. Contrary to the first flood, the contribution of Zone II increases during this second flood period, indicating an inversion of the trend. Finally, during the final state, the respective contributions of drains and zones is similar to those of pre-event conditions — even if discharge has doubled.

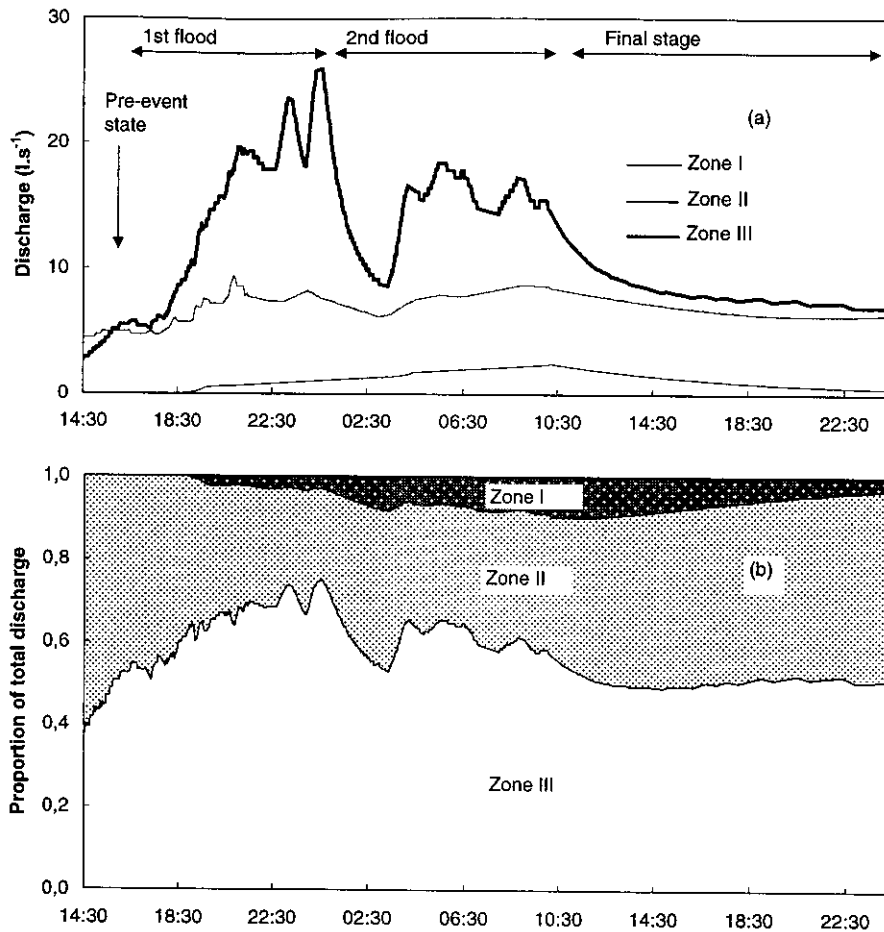


Fig. 6. Discharge variations of the hydrological zones (a) and of their relative contributions to streamflow (b) at the outlet during the 18–20th May storm event.

To summarise, for the whole event, Zone I only contributes for a very small part to the total volume of the flow ( $137 \text{ m}^3$  i.e. 5.5%). This weak volume ( $0.5 \text{ l m}^{-2}$ ) indicates the absence of overland runoff — except on the channel and on the tracks — in this upper part of the Strengbach basin. Zone II contributes for  $890 \text{ m}^3$  (i.e. 35.8%) to the total stream flow. This volume (corresponding to  $3.5 \text{ l m}^{-2}$ ) is mainly composed of baseflow, and is provided mostly by the ungauged flow  $QX_{II}$ . The contribution of Zone III to the total volume of the flow, is  $1457 \text{ m}^3$  (i.e. 58.7%), mainly composed of runoff flood and represents  $5.7 \text{ l m}^{-2}$ , provided mostly from the ungauged flow  $QX_{III}$  and from RUZS drain (Fig. 6).

These values indicate that, within the catchment: (i)

spatial contributions behave differently during the event; and (ii) if related to rainfall amount, the contributions can be negligible for some zones.

#### 4.2.2. Isotopic hydrograph separation: contribution of pre-event water

From the previous qualitative analysis, the isotope hydrograph separation has been performed using the event isotopic signature of the two rainfall events calculated by Eq. (10) and with a constant pre-event water signature ( $-9.45\text{‰}$ , stream baseflow value). Results obtained by the use of the two-component mixing model are shown in Fig. 8. The hydrograph separation indicates that the instantaneous event ranged from a minimum of 2% at the beginning of

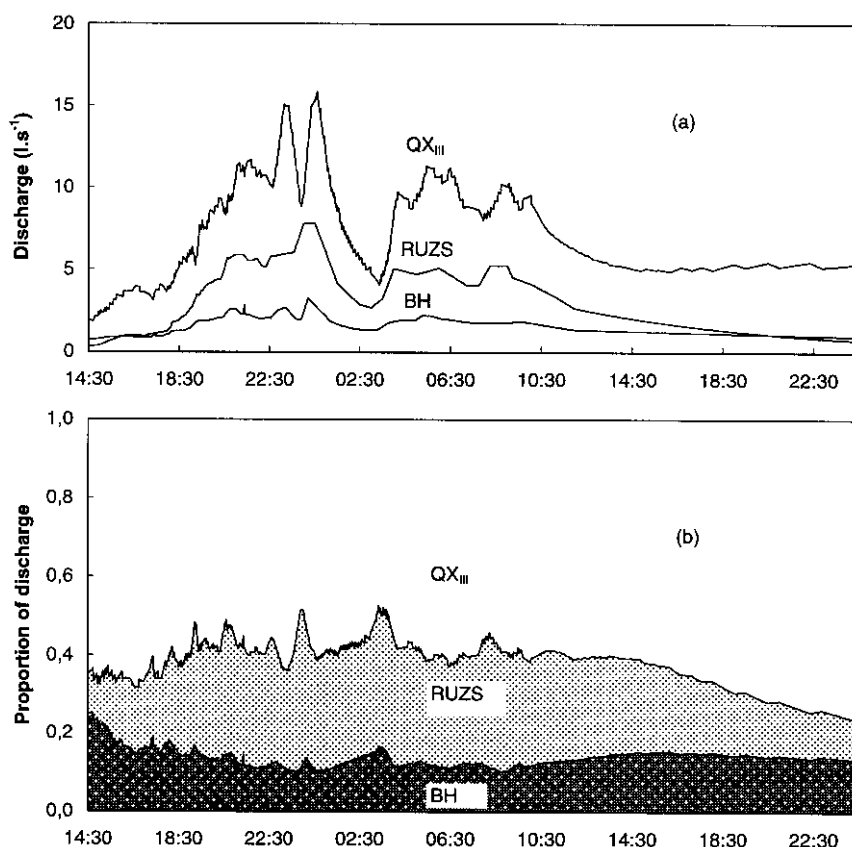


Fig. 7. Discharge variations of the main tributaries BH and RUZS and of the non-point flow ( $X_{III}$ ) (a) and of their relative contributions to zone III discharge (b) during the 18–20th May storm event.

the stormflow to a maximum value of 13% at the main peak flow. The calculation of the event contribution for the entire stormflow period is not possible since the isotopic hydrograph separation cannot be accomplished when the  $\delta$ -values of event water are equal or very close to that of pre-event water. Besides, it is assumed that a more 0.7‰ unit difference between old and new water is needed to differentiate the hydrologic contribution of the stormflow components (Ladouche, 1997). The periods with missing data are specified on Fig. 8. However, assuming that, the relative contributions of event and pre-event water remain constant during these periods, and identical to those calculated immediately before the missing data period, then the new water contribution estimated for the entire rainfall event is of  $9.5 \pm 3.5\%$ .

#### 4.2.3. Chemical hydrograph separation: contributive areas and reservoirs

##### (a) Determination of efficient tracers and end-members

In order to identify the contributing sources to the chemical composition of streamwater during the hydrological event, end-member mixing diagrams (Christophersen et al., 1990; Hooper et al., 1990) have been performed for major and trace chemical elements using the data of all sampled sites. Selected tracers used in end-member mixing diagrams are supposed to be conservative. Chemical parameters like conductivity,  $K^+$ ,  $Ca^{2+}$ ,  $Mg^{2+}$ ,  $Na^+$ ,  $Cl^-$ ,  $NO_3^-$ , alkalinity, ANC and silica are the most widely used in the literature for storm hydrograph separations (Pinder and Jones, 1969; Hill, 1993; Dewalle and Pionke, 1994; Robson and Neal, 1990; Robson et al.,

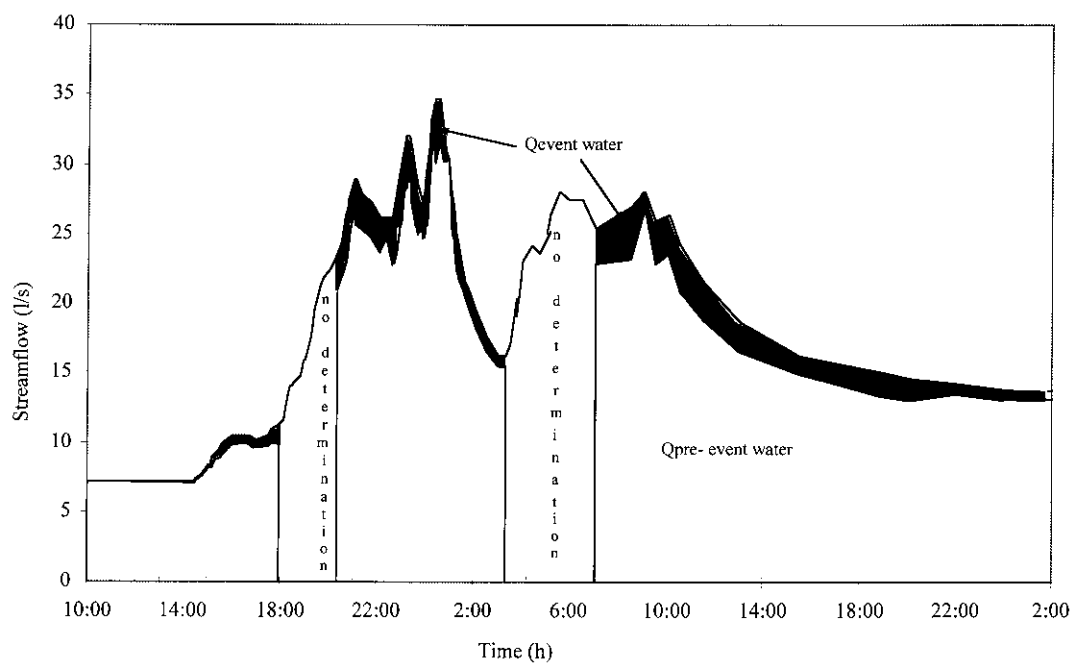


Fig. 8. Two-component (event/pre-event) hydrograph separation using  $^{18}\text{O}$  (a) and variation of their contributions to streamflow at the outlet (b) for the 18–20th May storm event.

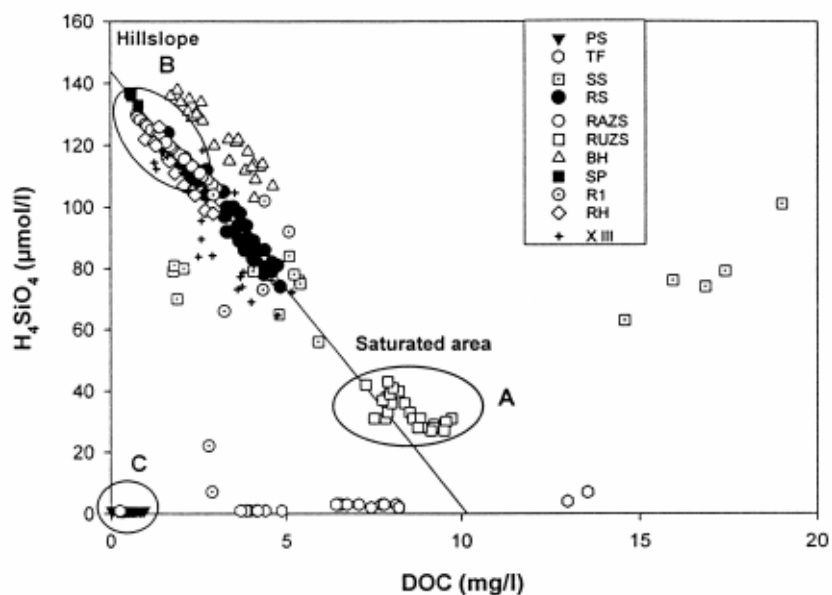


Fig. 9. Mixing diagram between DOC and silica for the different sampling sites during the 18–20th May storm event.

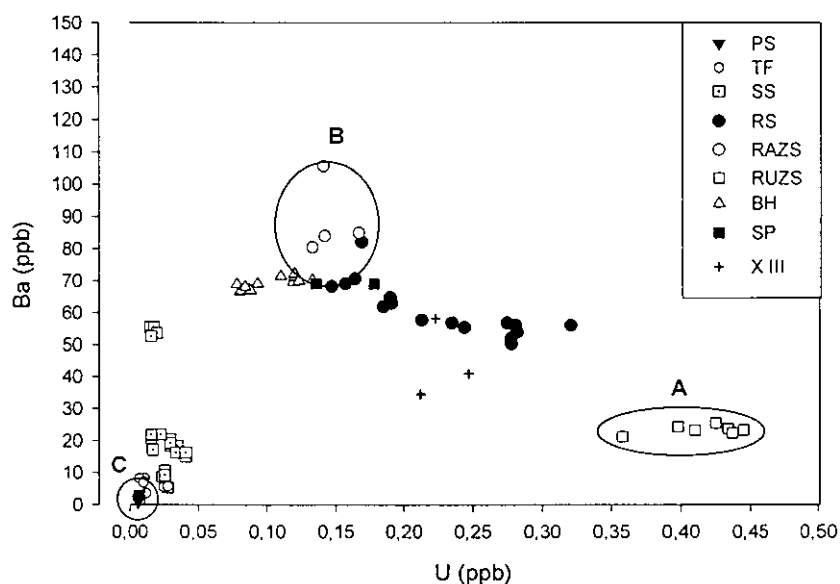


Fig. 10. Mixing diagram between Ba and U for the different sampling sites during the 18–20th May storm event.

1992; Elsenbeer et al., 1995; Soulsby, 1995; Neal et al., 1997). In our case study, silica, sodium, chloride, DOC, Rb, Sr, Ba and U, are considered as adequate. All other parameters either do not allow to discriminate different sources or do not present a clear relationship with discharge, because of various origins or different processes involved in the control of their chemistry (biological uptake and release, adsorption, desorption, precipitation...). Analysis of mixing diagrams — for assumed conservative elements at the storm event scale — show that streamwater at the outlet (RS) can be mainly explained by a linear mixing between two obvious end-members (A and B). This is particularly clear for example using  $\text{H}_4\text{SiO}_4$  and DOC (Fig. 9), and Ba and U (Fig. 10). Component A is characterised by high DOC and U, and low Si and Ba concentrations, and displays the signature of the upper horizons of the saturated areas (RUZS pattern). Component B (Figs. 9 and 10), with low DOC and U, and high Si and Ba contents, displays the signature of the deep layers of the hillslopes (as usually observed for silica: Kennedy et al., 1986; Maulé and Stein, 1990; Pionke et al., 1993; Hooper and Shoemaker, 1986). To our knowledge, DOC and U are not commonly used in hydrograph separation studies except Soulsby (1992, 1995) for DOC. Component

B is represented by RAZS and collects all the upper subcatchment rills, particularly the spring waters (SP) draining granite which characterise the type of waters mainly contributing to RAZS. BH is a little bit silica enriched (Fig. 9) mainly because it partly drains the small gneiss area.

According to hydrological measurements, 25–40% of the stream discharge is supplied by non-point flows from of the zone III (see Section 4.2.1). In order to assess the origin of all the contributing components to RS, an estimation of the chemical composition of this ungauged flow ( $X_{\text{III}}$ ) is performed. This chemical composition — identified using chemical tracers (major and trace elements) in a mass balance flux equation (see Eq. (3) where known concentrations were multiplied by corresponding discharges) —, varies during the event according to discharge variations.  $X_{\text{III}}$  concentration pattern is comparable to RS as seen in many major element mixing diagrams (Fig. 9), however, it presents slight deviation according to trace element combinations (Fig. 10). Even if  $X_{\text{III}}$  chemical composition is rather close to RS,  $X_{\text{III}}$  non-point flow cannot simply be explained by a linear mixing between components A and B (Figs. 9 and 10). The specific composition of this non-point flow indicates a small contribution of a more dilute



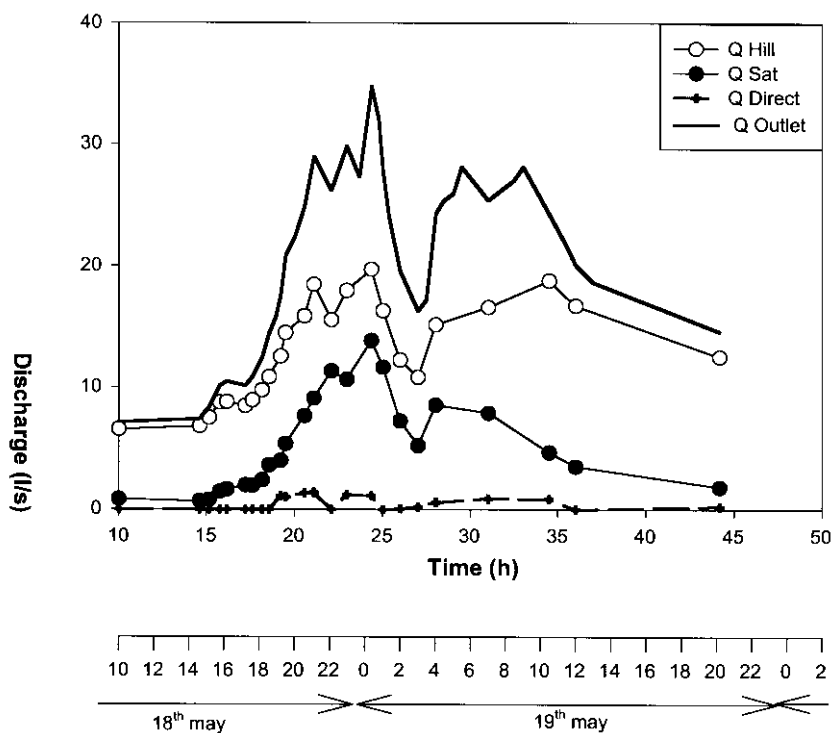


Fig. 11. Three-component (deep layers of the hillslopes ( $Q_{\text{hill}}$ ), surface layers of the saturated areas ( $Q_{\text{sat}}$ ) and diluted end-member ( $Q_{\text{direct}}$ )) hydrograph separation using DOC and silica for the 18–20th May storm event.

end-member, which can be associated to rainwater PS (component C). Several mixing diagrams involving other trace or major elements also confirm this pattern. Moreover, it is important to note — as also confirmed by many mixing diagrams — that SS and TF measured under the spruce stands in the upper subcatchment (Fig. 1) are not involved directly and significantly on the mixing lines. Consequently, during this storm event, their direct contribution to the chemical composition of the mainstream water at the outlet, remains very weak.

(b) Respective contributions of areas and reservoirs

Chemical hydrograph separation (Pinder and Jones, 1969; Hall, 1970) is performed using DOC and silica (Fig. 11), according to the chemical pattern described above. These tracers are considered as conservative in this catchment since at the event scale no biological activity could influence silica behaviour and DOC is mainly composed of refractory DOC. Trace elements could not be used for hydro-

graph separation because of shortage of measurements. The objective is to separate the streamflow components into contributing areas, impossible to identify using direct hydrological measurements within the whole catchment.

The chemical characteristics of RUZS (representing the upper layers of the saturated areas: component A), RAZS (associated to the major contribution of the deep layers of the hillslope: component B) and rainwater (representing the highly diluted end-member: component C), are used to separate step by step streamflow into three components, according to Eqs. (7) and (8). Since springwaters were not sampled step by step during the event, RAZS is chosen as to represent the hillslope component in the hydrograph separation. Hence, contrary to what is classically done in the literature, the variations of concentrations in the different reservoirs or contributing areas could have been taken into account in the hydrograph separation.

Fig. 11 represents the respective contributions based on calculations using silica and DOC: the deep layers of the hillslope ( $Q_{\text{hill}}$ ), the upper layers of the saturated area ( $Q_{\text{sat}}$ ), and the rain water ( $Q_{\text{direct}}$ ). The results indicate that surface waters draining the deep layers of the hillslope (70% of total stream flow) mainly contribute to the total stream discharge ( $Q_{\text{hill}}$ , Fig. 11). Nevertheless, this contribution is slightly lower during the first period (68%) of the event than during the second one (77%). The contribution of the dilute end-member to streamflow is found very low (from 0 to 4%, 2% as a mean). These estimations are consistent with those obtained taking into account other major elements or isotopic tracers (90% of pre-event waters). Indeed, we can assess that the major part of the hillslope contribution is dominated by pre-event water.

A little part of the saturated area is included in the RAZS upper subcatchment II (hydrological zones I and II, see Fig. 1), therefore this end-member is not pure. A chemical hydrograph separation is then performed for what is supposed to represent the deep layers of the hillslope. The objective is to determine the respective contributions of deep water flow (spring water end-member) and of surface saturated flow (saturated area end-member). In this calculation, we consider only two components assuming that the influence of the dilute end-member can be neglected in the upper part of the catchment. The mean composition of the end-members is supposed to be constant during the event (SP:  $130 \mu\text{mol l}^{-1}$  for silica and  $1 \text{ mg l}^{-1}$  for DOC; RUZS:  $30 \mu\text{mol l}^{-1}$  for silica and  $10 \text{ mg l}^{-1}$  for DOC), since no significant variation in spring water chemical composition is observed.

On average, according to DOC and silica, respectively, 87% and 85% of the waters really originate from deep layers of the hillslopes in the upper subcatchment II, whereas the remaining 13 and 15% are characteristic of the surface waters from the small upper part of the saturated areas. The contribution of these upper saturated areas is, respectively, 10–12% during the first part of the event and reaches between 15 and 17% during the second part.

Hence, if we consider that 86% of RAZS only originates from the deep layers of the hillslope rather than 100%, the estimation of the deep layers of the hillslope contribution to the stream outlet RS may be overestimated by about 6%.

## 5. Discussion and conclusions

This study associates three different approaches to trace the origin of the water participating to stream-flow generation. However, isotopic and chemical tracers could not be combined in a unique and single water component separation since each of them brings a particular and different information. Table 3 summarises the respective contributions of the hydrological zones I–III, of the event water and of the contributive areas for instantaneous samplings corresponding to the most significant periods of the hydrological event. It is by considering these different results that the hydrological pathways as well as the origin of the water can be determined.

As a whole, during such a major type of event following relatively dry hydrological conditions, chemical and isotopic hydrograph separations indicate that the water from the deep layers of the hillslope as well as the pre-event contributions to the total streamflow are dominant (as shown in other similar catchments, Hooper and Shoemaker, 1986; Robson and Neal, 1990 as examples) (Table 3). The chemical tracers (DOC and silica) allowed us to quantify the contributions both in the hydrological subcatchment RAZS (i.e. including Zones I and II) and at the outlet (i.e. including Zones I–III). The direct contribution of rainwater is negligible whereas the upper layers of the saturated areas play a significant role particularly at the maximum of the first event.

During the recession stage preceding the event (Table 3), water is mainly composed of “old-water” draining the deep layers of the superficial formations in Zones I and II (i.e. the upper subcatchment).

During the first flood event (Table 3), at the maximum, saturated areas mainly located in the hydrological Zone III response to the rain probably by overland runoff then by groundwater ridging as indicated by piezometer water level and isotopic data. Rainwater penetrates in the coarse texture soils of the catchment unsaturated slopes and contribute to reconstitute the water storage of the catchment. These waters are then mixed with pre-existing waters. The contribution of the upper hillslope in Zone I is very weak because soils are dry and reconstitute their storages. Most of the runoff comes from the down stream part of the basin. On the opposite, rainwater (i.e. event water) falling on the saturated areas, mainly

Table 3

Respective contributions of water components during significant periods of the 18–20 May 1994 event after hydrological measurements,  $^{18}\text{O}$ , silica and DOC hydrograph separations (UL: upper layers; DL: deep layers)

%	Respective contributions			
	Recession period before first event 11:35	First maximum first flood event 21:00	Second maximum second flood event 10:00	Recession period after second event 15:30
Hydrological zones				
I	0	2	9	8
II	64	30	33	43
III	36	67	58	49
$^{18}\text{O}$ separation				
Event water	0	$10.5 \pm 0.8$	$13.5 \pm 1.1$	$8.7 \pm 0.7$
Pre-event water	100	$89.5 \pm 6.7$	$86.5 \pm 6.8$	$91.3 \pm 7.2$
$\text{H}_4\text{SiO}_4$ separation				
UL saturated areas	4	39	25	15
DL hillslopes	96	61	75	85
DOC separation				
UL saturated areas	10	30	18	21
DL hillslopes	90	70	82	79

reacts on the upper layers of the saturated areas of zone III, mix rapidly with pre-existing waters and participate instantaneously to the total streamflow. Even if these saturated areas are representing only 2% of the whole catchment area — and occupying mainly the hydrological zone III, — about 30% of the waters at the outlet originate from their surface layers as indicated by chemical tracers. The increase of Zone III contribution and of event water proportion reinforce this hypothesis. However, as a whole the pre-event water from the deep layers of the hillslope remains highly dominant.

At the maximum discharge of the second event, the increasing contribution of Zone II and stream flow in Zone I as well as piezometer levels in the saturated area let us think that lateral piston could have produced water level ridging in the saturated areas (mainly in zone III). The proportion of event waters becomes relatively more important whereas waters from deep layers of the hillslope are proportionally higher than during the first event as indicated by chemical tracers. The waters from the deep layers of the hillslopes in the upper subcatchments now reach the stream. This contributes to water supply in the saturated areas which are connected to the stream. Hence the contribution of

the upper layers of these areas to stream flow becomes lower.

In the final stage, Zones II and III contribute in the same proportion to streamflow, event water proportion goes reducing whereas the deep layers of the hillslopes become highly dominant. This indicates that rainwater which fall in the upper part of this catchment does not participate directly to the stream flow generation during such an event. However, this water contributes to reconstitute the catchment water storage particularly in the deep layers of the hillslope superficial formations. In the final stage, this water is released mainly in Zones II and III by lateral deep flow. The final state is characterised by a balanced contribution between aquifers located in moraine (Zone II) and downslope (Zone III).

This approach points out the strength of the chemical (both trace and major elements) and isotopic tracers to identify the origin of water pathways in such environmental conditions. In the literature, much hydrograph separations were performed in similar catchments (granitic, forested), using specific tracers. However, the simultaneous use of different naturally occurring tracers enables a quality check in the reliability of the hydrograph separation. Thanks to the simultaneous measurements of the different

water contributions inside the catchments (particularly in saturated areas), the end-members and their chemical and isotopic evolution have been taken into account step by step during the event. Such an effort based on complementary approaches in time and space should be recommended in hydrological studies because of the specificity of the sites and of the events according to prevailing hydrological conditions.

Moreover, except on a hydrological point of view, the geochemical characteristics of saturated areas and consequently their geochemical influences on stream-water chemistry are so far poorly documented in the literature.

## Acknowledgements

This work has been carried out within the DBT II "Fleuves et Erosion" research programme supported by the INSU/CNRS. The authors are also grateful to all participants in the field (Mathieu Ayh  re, Nielza Dos Castros, Brahim Ezzahar, Laurent Fischer, Selma Groot, Sylvain Huon, Barbara Laing, Antoine Millet, Patricia Richard, Serguie Sokolev and Ren   Winter-oeken) and in the laboratory (Yvette Hartmeier, Daniel Million, Gerard Krempf and Wolfgang Ludwig) for their contribution which allows this study to progress in good conditions.

## References

- Buttle, J.M., 1994. Isotope hydrograph separations and rapid delivery of pre-event water from drainage basins. *Prog. Phys. Geogr.* 18 (1), 16–41.
- Christophersen, N., Neal, C., Richard, H., Vogt, R.D., Andersen, S., 1990. Modelling streamwater chemistry as a mixture of the soil-water end-members — a step towards second generation acidification models. *J. Hydrol.* 116, 307–320.
- Coleman, M.L., Shepherd, T.J., Durham, J.J., Rouse, J.E., Moore, G.R., 1982. Reduction of water with zinc for hydrogen isotope analysis. *Anal. Chem.* 54, 993–995.
- Dambrine, E., Ulrich, E., C  nac, N., Durand, P., Gauquelin, T., Mirabel, P., Nys, C., Probst, A., Ranger, J., Z  phoris, M., 1995. Atmospheric deposition in France and possible relation with forest decline. In: Landmann, G., Bonneau, M. (Eds.). *Forest Decline and Atmospheric Deposition Effects in the French Mountains — Part 3*. Springer, Berlin/Heidelberg/New York, pp. 203–225.
- Dewalle, D.R., Pionke, H.B., 1994. Streamflow generation on a small agricultural catchment during autumn recharge: 2. Storm flow periods. *J. Hydrol.* 163, 23–42.
- Durand, P., Neal, M., Neal, C., 1993. Variation in stable oxygen isotope and solute concentrations in small sub-Mediterranean montane streams. *J. Hydrol.* 144, 283–290.
- Epstein, S., Mayeda, T., 1953. Variation of  $^{18}\text{O}$  content of waters from natural sources. *Geochim. Cosmochim. Acta.* 4, 224–231.
- El Gh  Mari, A., 1995. Etude p  trographique, min  ralogique et g  ochimique de la dynamique d'alt  ration d'un granite soumis aux d  p  ts atmosph  riques acides (bassin versant du Strengbach, Vosges, France): m  canisme, bilan et mod  lisation. Th  se de doctorat, Universit   Louis Pasteur, Strasbourg, 200pp.
- Elsenbeer, H., Lorieri, D., Bonell, M., 1995. Mixing model approaches to estimate storm flow sources in an overland flow-dominated tropical rain forest catchment. *Water Resour. Res.* 9, 2267–2278.
- Gonfiantini, R., 1978. Standards for stable isotope measurements in natural compounds. *Nature* 271, 534–536.
- Hall, F.R., 1970. Dissolved solids-discharge relation ships 1. Mixing models. *Water Resour. Res.* 6 (3), 845–850.
- Hewlett, J.D., Hibbert, A.R., 1967. Factors affecting the response of small watersheds to precipitation in humid areas. In: Sopper, W.E., Lull, H.M. (Eds.). *Forest Hydrology*. Pergamon, Oxford, pp. 275–290.
- Hill, A.R., 1993. Base cation chemistry of storm runoff in a forested headwater wetland. *Water Resour. Res.* 29 (8), 2663–2675.
- Hooper, R.P., Shoemaker, C.A., 1986. A comparison of chemical and isotopic hydrograph separation. *Water Resour. Res.* 22 (10), 1444–1454.
- Hooper, R.P., Christophersen, N., Peters, J., 1990. Modelling streamwater chemistry as a mixture of soilwater end members—an application to the Panola mountain catchment, Georgia, USA. *J. Hydrol.* 116, 321–343.
- Idir, S., 1998. Etude G  ochimique des crues du bassin versant du Strengbach (Vosges): Origine des   coulements et contribution aux flux d'  l  ments majeurs dissous export  s. Th  se Universit   Louis Pasteur de Strasbourg, 266pp.
- Kendall, C., McDonnell, J.J., 1993. Effect of intrastorm isotopic heterogeneities of rainfall, soil water and groundwater on runoff modeling. *Tracers in Hydrology, Proceedings of the Yokohama Symposium, IAHS*, pp. 41–48.
- Kennedy, V.C., Kendall, C., Zellwegger, G.W., Wyerman, T.A., Avanzino, R.J., 1986. Determination of the components of stormflow using water chemistry and environmental isotopes, Mattole river basin, California. *J. Hydrol.* 84, 107–140.
- Ladouche, B., 1997. Etude des flux hydriques par le tra  age isotopique naturel    l'  chelle d'un bassin forestier (Strengbach, Vosges). Th  se Doct., Univ. Pierre et Marie Curie, 194pp.
- Landmann, G., Bonneau, M., 1995. *Forest Decline and Atmospheric Deposition Effects in the French Mountains*. Springer, Berlin/Heidelberg/ New York (461pp.).
- Latron, J., 1990. Caract  risation g  omorphologique et hydrologique du bassin versant du Strengbach (Aubure). M  moire de Ma  trise, UFR de G  ographie, CEREG, Universit   Louis Pasteur, Strasbourg I, 96pp.
- Laudon, H., Slaymaker, O., 1997. Hydrograph separation using stable isotopes, silica and electrical conductivity: an alpine example. *J. Hydrol.* 201, 82–101.
- Matzner, E., 1986. Deposition/canopy-interaction in two forest

- ecosystems of northwest Germany. In: Georgii, H.W. (Ed.). *Atmospheric Pollutants in Forest Areas*. Reidel, Dordrecht, pp. 247–462.
- Maulé, C.P., Stein, J., 1990. Hydrologic flow path definition and partitioning of spring meltwater. *Water Resour. Res.* 26 (12), 2959–2970.
- McDonnell, J.J., Bonell, M., Stewart, M.K., Pearce, A.J., 1990. Deuterium variations in storm rainfall: implication for stream hydrograph separation. *Water Resour. Res.* 26 (3), 455–458.
- Millet, A., Bariac, T., Ladouche, B., Mathieu, R., Grimaldi, C., Grimaldi, M., Hubert, P., Mollicova, H., Bruckler, L., Vallès, V., Bertuzzi, P., Brunet, Y., 1998. Influence de la déforestation sur le fonctionnement hydrologique de petits bassins versants tropicaux. *Rev. Sci. Eau* 1, 63–86.
- Neal, C., Hill, T., Hill, S., Reynolds, B., 1997. Acid neutralising capacity measurements in surface and ground waters in the Upper River Severn, Plynlimon: from hydrograph splitting to water flow pathways. *Hydrol. Earth Syst. Sci.* 3, 687–696.
- Pinder, G.F., Jones, J.F., 1969. Determination of the groundwater component of peak discharge from the chemistry of total runoff. *Water Resour. Res.* 5 (2), 438–445.
- Pionke, H.B., Gburek, W.J., Folmar, G.J., 1993. Quantifying storm-flow components in a Pennsylvania watershed when  $^{18}\text{O}$  input and storm conditions vary. *J. Hydrol.* 148, 169–187.
- Probst, A., Viville, D., 1997. Bilan hydrogéochimique d'un petit bassin versant forestier des Vosges granitiques en Alsace: Le bassin amont du Strengbach à Aubure (Haut-Rhin). Rapport d'activité scientifique ZAFA 1.3 de l'IFARE (Institut Franco-Allemand de Recherche sur l'Environnement), Région Alsace, période 1996–1997, 6pp.
- Probst, A., Dambrine, E., Viville, D., Fritz, B., 1990. Influence of acid atmospheric inputs on surface water chemistry and mineral fluxes in a declining spruce stand within a small granitic catchment (Vosges massif, France). *J. Hydrol.* 116, 101–124.
- Probst, A., Viville, D., Fritz, B., Ambroise, B., Dambrine, E., 1992. Hydrochemical budgets of small forested granitic catchment exposed to acid deposition: The Strengbach catchment case study (Vosges massif, France). *Water Air Soil Pollut.* 62, 337–347.
- Probst, A., Fritz, B., Viville, D., 1995. Mid term trends in acid precipitation, streamwater chemistry and elements budgets in the Strengbach catchment (Vosges mountains, France). *Water, Air and Soil Pollution* 79, 39–59.
- Probst, A., El Gh' Mari, A., Aubert, D., Fritz, B., Mc Nutt, R.H., 2000. Strontium as tracer of weathering processes in a silicate catchment polluted by acid atmospheric inputs, Strengbach, France. *Chem. Geol.* 170, 203–219.
- Robson, A., Neal, C., 1990. Hydrograph separation using chemical techniques: an application to catchments in Mid-Wales. *J. Hydrol.* 116, 345–363.
- Robson, A., Neal, C., Christophersen, J.S., Hill, S., 1992. Short-term variations in rain and stream water conductivity at a forested site in mid-Wales-implications for water movement. *Sci. Total Environ.* 119, 1–18.
- Rodhe, A., 1987. The origin of streamwater traced by oxygen-18. Uppsala Univ., Dept. Phys. Geogr. Div. Hydrol. Report series A N° 41, Uppsala (S), 260pp. + appendix 73pp.
- Sklash, M.G., Farvolden, R.N., 1979. The role of groundwater in storm runoff. *J. Hydrol.* 43, 45–65.
- Soulsby, C., 1992. Hydrological controls on acid runoff generation in an afforested headwater catchment at Llyn Brianne, Mid-Wales. *J. Hydrol.* 138, 431–448.
- Soulsby, C., 1995. Contrasts in storm event hydrochemistry in an acidic afforested catchment in Upland Wales. *J. Hydrol.* 170, 159–179.
- Viville, D., Ambroise, B., Probst, A., Fritz, B., Dambrine, E., Gelhaye, D., Deloze, C., 1988. Le bassin versant du Strengbach à Aubure (Haut-Rhin, France) pour l'étude du dépérissement forestier dans les Vosges (Programme DEFORPA). I-Equipement climatique, hydrologique, hydrochimique. In: Mathy, P. (Ed.). *Proceedings of the international symposium Air Pollution and Ecosystems*, Grenoble 18–22 mai 1987. D. Riedel, Bruxelles, pp. 823–828.
- Wels, C., Cornett, R.J., Lazarete, B.D., 1991. Hydrograph separation: a comparison of geochemical and isotopic tracers. *J. Hydrol.* 122, 53–274.
- Zimmerman, U., Ehhalt, D., Münnich, K.O., 1967. Soil water movement and evapotranspiration: changes in the isotopic composition of the water. *Isotopes in Hydrology*, Proc. symp., I.A.E.A., Vienne, pp. 567–585.